Chapter 3

Becker-Döring Theory and the Droplet Model

©2012 by W. Klein, Harvey Gould, and Jan Tobochnik
1 October 2012

3.1 Introduction

As we have emphasized, the theories presented in Chapters 1 and 2 have limited validity. The aim of the next few chapters is to develop theories for nucleation, spinodal decomposition, and continuous ordering that have a wider range of validity. What is wrong with the theories we have discussed so far? In this chapter we will answer this question in the context of the classical theory of nucleation.

It should be stressed that experimental data, that is to say, real experiments do not detect the critical droplets in most materials except for colloidal and polymer systems. Experimentalists usually measure nucleation rates by counting the number of droplets that they can detect per unit volume per unit time. However, because these droplets are much bigger than the critical droplets, experimentalists must hope that the density of the droplets is low enough so that there is no coalescence during the growth phase. With this understanding we point out that there are many experiments that agree with the classical theory; that is, the nucleation rate scales with quench depth as predicted in Eqs. (1.14) and Eq. (1.15). There are several experiments where the quench depth dependence is not predicted by the classical theory. Of course it is very difficult to control all of the factors in real experiments so it is difficult to know just how bad the disagreement is with the classical theory. These issues will be discussed in Chapter 4.

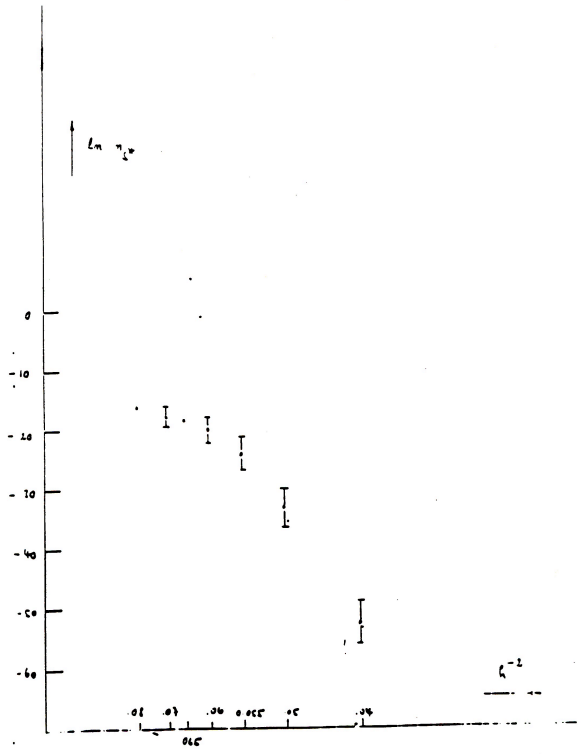

Figure 3.1: Plot of the logarithm of the nucleation rate as a function of h^{-2} for the $d = 3$ Ising model at $T = 0.86T_c$.

There are other reasons to believe that the classical theory as presented in Chapter 1 is incomplete and not universally valid. In Fig. 3.1 we show a plot of the log of the nucleation rate as a function of h^{-2} for the same Ising model [Heermann, et al. 1984] as in Fig. 1.11 with the only difference being the temperature. The temperature in Fig. 1.11 is $0.59T_c$ and that in Fig. 3.1 is $0.86T_c$, much closer to coexistence. Note the curvature in Fig. 3.1 as well as the difference in the magnitude of the rates. In Fig. 3.2 we plot the log of the nucleation rate as a function of h^{-2} for the same Ising model as in Fig. 1.11 but with a different dynamics [Ray and Wang 21990].The crosses, open circles and triangles are taken for different system sizes using an algorithm known as the Swendsen-Wang algorithm [Swendsen and Wang 1987]. The only difference between the Swendsen-Wang dynamics and the Metropolis algorithm is that clusters rather than single spins are flipped. Note the change in the position of the line of data. It appears that these two simple changes; temperature and dynamics lead to a change in the nucleation rate that is not predicted by the simple theory in Chapter 1.

There are other problems with the simple theory as well. For example, there is a

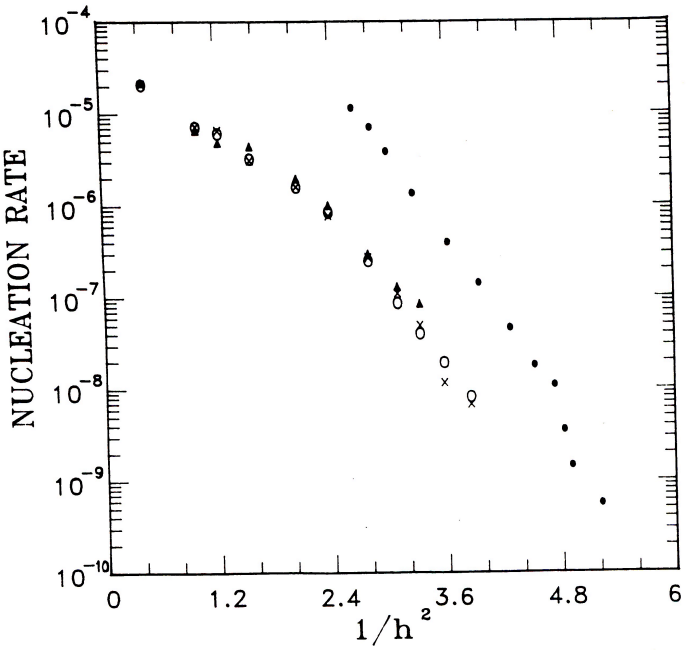

Figure 3.2: Plot of the logarithm of the nucleation rate as a function of h^{-2} for a $d = 3$ Ising model at $0.59T_c$ simulated with the Swendsen-Wang cluster algorithm (top curve). The closed circles are same as the data shown in Fig. 1.11 and are shown to facilitate comparison.

strong assumption about the shape of the critical droplet. We would like to see this assumption obtained beginning from basic principles. Secondly, it is not clear that this assumption is valid. For example, let us return to the mean-field model discussed in Chapter 1. Mean-field descriptions of Ising models become exact in the limit of long-range interactions [Penrose and Lebowitz 1976]. That is, spinodals are precisely defined for long-range models. This property is illustrated in Fig. 3.3 where we have plotted the inverse isothermal susceptibility for Ising models with different interaction ranges [Heermann et al. 1982]. The interaction region has each spin at the center of a cube ($d = 3$) or square ($d = 2$) of linear dimension ℓ. The spin at the center of the cube has an interaction that is zero with spins outside of the cube and is a constant K for each spin in the cube with equal strength. The constant K is given by

$$K = \frac{J}{k_B T q}, \tag{3.1}$$

where $q = \ell^d$ is the number of spins with which one spin interacts. This model is known as the Domb-Dalton model [Domb and Dalton 1966].

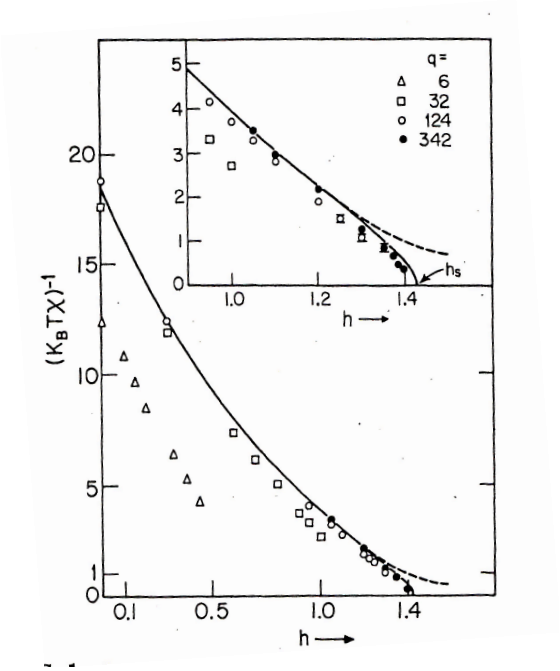

Figure 3.3: Plot of the the inverse isothermal susceptibility versus the magnetic field for the $d = 3$ Ising model for various interaction ranges. The solid line is the exact mean-field solution. The parameter q is the number of spins with which a given spin interacts; $q = 6$ corresponds to nearest neighbor interactions on a simple cubic lattice.

For $q = 6$ the interaction is nearest neighbor in the simple cubic lattice used in our simulations. Note that there is really no sign of a spinodal in the nearest neighbor model. As q and hence the interaction range increases, the model becomes more mean-field as can be seen by comparing the data to the solid line which is the exact solution as $q \to \infty$. The isothermal compressibility diverges as the spinodal is approached similar to the behavior at a critical point. The surface tension will also vanish [Domb and Dalton 1966]. This result presents two difficulties for the classical theory. First, the surface tension cannot prevent nucleation if it is vanishing. Second, droplets, or any large fluctuations, cannot be compact objects with a distinguishable surface and interior in the vicinity of a critical point [Klein and Unger 1983].

Another problem we need to face is the nature of the metastable state itself. In mean-field theories the free energy and equations of state in the metastable state are analytic continuations of their stable state counterparts. Is this property still valid for systems with finite range forces. If not, how do we describe the metastable state?

For all of the reasons we have discussed we need to reexamine the theory of metasta-

bility and nucleation. In the next few chapters we will return to this problem with various techniques and examine some of the complications and subtleties.

3.2 Becker-Döring theory

To understand the problem with the simple approach in Chapter 1 we need to return to it and reformulate it in more precise terms. Such a reformulation was done by Becker and Döring in 1935 [Gunton et al. 1983]. The Becker-Döring theory is not without its own assumptions, but it is a more fundamental theory than the one discussed in Chapter 1.

The basic assumption of the theory is that clusters with ℓ monomers grow and decay via an evaporation-condensation mechanism where the droplet or cluster gains or loses a single molecule. Consequently the theory neglects coalesence and fission. The time derivative of the number of clusters of size ℓ, $n_\ell(t)$, can be written as

$$\frac{\partial n_\ell(t)}{\partial t} = J_{\ell-1} - J_\ell, \tag{3.2}$$

where

$$J_{\ell-1} - J_\ell = \big(R_{\ell-1} n_{\ell-1}(t) - R'_\ell n_\ell(t)\big) - \big(R_\ell n_\ell(t) - R'_{\ell+1} n_{\ell+1}(t)\big) \tag{3.3}$$

is the rate per unit volume at which droplets of size ℓ are created. The term $R_{\ell-1} n_{\ell-1}$ is the rate per unit volume at which droplets with $\ell - 1$ monomers gain a monomer to become droplets with ℓ monomers and $R'_\ell n_\ell$ is the rate at which droplets with ℓ monomers lose a monomer to become droplets with $\ell - 1$ monomers. The second assumption of Becker-Döring is embodied in Eq. (3.3). Namely, the rates of gain or loss of monomers from droplets of size ℓ are proportional to n_ℓ.

We can relate R and R' to another assumption. The assumption is that the system is very close to metastable equilibrium. What is meant by "very close" will be defined shortly. At equilibrium, either stable or metastable, the number of droplets or clusters of size ℓ is given by equilibrium fluctuation theory. Namely

$$\overline{n}_\ell = e^{-\Delta F_\ell / k_B T}, \tag{3.4}$$

where ΔF_ℓ is the free energy cost of a cluster of size ℓ. At equilibrium the number of droplets of size ℓ is a constant so that the time derivative of $n_\ell(t) = 0$, which implies that

$$R_{\ell-1} e^{-\Delta F_{\ell-1}/k_B T} = R'_\ell e^{-\Delta F_\ell / k_B T}. \tag{3.5}$$

Equation (3.5) relates $R_{\ell-1}$ to R'_ℓ but we still must determine R_ℓ and justify the equilibrium assumption used to obtain Eq. (3.5). Before doing so we will make the approximation that ℓ can be treated as a continuous variable. The justification for this

assumption is twofold. First the droplets change only by increasing or decreasing ℓ by 1 and for all droplets of interest $\ell \gg 1$. Having said that we point out that we will consider droplets with small ℓ, but that extension will not change the conclusions in any substantive way. We now write

$$\frac{\partial n_\ell(t)}{\partial t} = -\frac{J_\ell - J_{\ell-1}}{\Delta\ell} = -\frac{\partial J_\ell}{\partial \ell}, \tag{3.6}$$

where $\Delta\ell = 1$ is treated as an infinitesimal and J_ℓ is given in the second bracket on the right-hand side of Eq. (3.3).

From Eqs. (3.3) and (3.5) we have

$$-J_\ell = R_\ell\, n_\ell(t) - R_\ell\, e^{-\frac{\Delta F_\ell - \Delta F_{\ell+1}}{k_B T}} n_{\ell+1}(t). \tag{3.7}$$

We expand the exponential to first order and obtain

$$-J_\ell = R_\ell\big[n_\ell(t) - n_{\ell+1}(t)\big] + \frac{R_\ell}{k_B T}\big[\Delta F_\ell - \Delta F_{\ell+1}\big] n_\ell(t), \tag{3.8}$$

where we have set $n_{\ell+1}(t) = n_\ell(t) + \Delta n_\ell$ equal to n_ℓ. We again treat $\Delta\ell = 1$ as an infinitesimal and use Eq. (3.6) to obtain

$$\frac{\partial n_\ell(t)}{\partial t} = \frac{\partial}{\partial \ell}\left[\frac{R_\ell}{k_B T}\frac{\partial \Delta F_\ell}{\partial \ell} n_\ell(t) + R_\ell \frac{\partial n_\ell(t)}{\partial \ell}\right]. \tag{3.9}$$

We now return to the question of determining R_ℓ. We will again assume that the droplets of interest are compact so that the rate is proportional to the surface area:

$$R_\ell \propto \ell^{(d-1)/d}. \tag{3.10}$$

We should not necessarily expect this assumption to hold near critical points or spinodals where the vanishing of the surface tension could lead to a different expression.

We now address the question of what it means to be very close to equilibrium. Note that $\overline{n}_\ell$ as defined in Eq. (3.4) is a solution to Eq. (3.9). Moreover from Eqs. (3.6) and (3.9) the condition $n_\ell(t) = \overline{n}_\ell$ leads to the vanishing of J_ℓ. A moment of reflection leads to the conclusion that this solution is not the one we wish. We do not want $J_\ell = 0$, which would imply that there is no "flow" of droplets from small ℓ to large. We want to describe the situation where there is a very small flow. If the flow is too large, the density will be high enough so that the droplets will interact. Moreover, the background would not be in metastable equilibrium.

The way around this dilemma is to realize that if the lifetime of the metastable state is large, so that the density of critical droplets is small, there will be a time interval during which droplets will go critical at a constant rate, yet their number will be so small that the

effect on the background is negligible. We use this idea to define a steady state condition. We postulate the existence of a steady state solution n_ℓ^s such that $\partial n_\ell^s(t)/\partial t = 0$, but $J_\ell = I \neq 0$, where I is a constant. We impose this condition by requiring that

$$\lim_{\ell\to 0} n_\ell^s = \overline{n}_\ell \text{ and } \lim_{\ell\to\infty} n_\ell^s = 0. \tag{3.11}$$

These boundary conditions, usually referred to as the source and sink conditions, can be viewed physically as taking droplets that grow beyond some critical size, breaking them up, and returning them to the background to keep $n_\ell(t) \sim \overline{n}_\ell$ for small ℓ.

The solution of Eq. (3.9) that satisfies these conditions is

$$n_\ell^s = I\int_\ell^\infty \frac{\overline{n}_\ell}{R_{\ell'}\overline{n}_{\ell'}} dl' \tag{3.12}$$

and

$$I^{-1} = \int_0^\infty \frac{dl}{R_\ell \overline{n}_\ell}, \tag{3.13}$$

as can be seen by substitution. The form of $\overline{n}_\ell$ is given in Eq. (3.4).

Let us consider the Ising model for which

$$\Delta F_\ell = h\ell + \sigma\ell^{(d-1)/d}. \tag{3.14}$$

From Eqs. (3.4), (3.10), (3.13), and (3.14) the inverse of the nucleation rate is

$$I^{-1} = \int_0^\infty \frac{\exp\big[-|h|\ell + \sigma\ell^{\frac{d-1}{d}}\big]}{\ell^{\frac{d-1}{d}}} d\ell, \tag{3.15}$$

where the magnetic field h is negative because the system is in the metastable state. We now define the variable

$$t \equiv \frac{|h|^d}{\sigma^d}\ell. \tag{3.16}$$

With Eq. (3.16), Eq. (3.15) becomes

$$I^{-1} = \frac{\sigma}{|h|}\int_0^\infty \frac{e^{-\frac{1}{k_BT}\frac{\sigma^d}{|h|^{d-1}}(t - t^{\frac{d-1}{d}})}}{\ell^{\frac{d-1}{d}}} dt. \tag{3.17}$$

Near the coexistence curve that is, $h \sim 0$, the integral in Eq. (3.17) can be done with the method of steepest descent. We obtain

$$I = \frac{|h|}{\sigma}\Big(\frac{d-1}{d}\Big)^{d-1}\Big[\frac{\sigma^d(d-1)}{d^2 k_BT|h|^{d-1}}\Big]^{1/2} e^{-\frac{\sigma^d(d-1)^{d-1}}{k_BT|h|^{d-1}d^d}}. \tag{3.18}$$

Note that the saddle point value of $t \propto (\sigma/|h|)^d$ is the droplet critical radius of Chapter 1 raised to the power d.

Equation (3.18) should be compared with the expression for τ^{-1}, where τ is given in Eq. (1.15). Note that the exponential terms are the same, but in Eq. (3.18) we have also obtained an expression for the prefactor to the exponential. We have also made precise something that was glossed over in Chapter 1, namely that the nucleation rates we are considering in both chapters are steady state rates. However, there are still problems. For example, the dependence on the conservation laws is not clear. We started with Eq. (3.2) which has no order parameter conservation, and it is not clear at this point how to include it, if it is needed. A second point is that the structure of the droplet is not obtained from this theory. At best it is put in by hand in Eq. (3.10). For these reasons we need something better than the Becker-Döring theory. To facilitate the development of a better theory we next look at the classical droplet model.

3.3 Classical droplet model

In this section we will consider a system at low temperature that consists of a uniform background of spins and excitations or fluctuations consisting of compact objects which are assumed to be sufficiently rare so that their interactions can be neglected. However, these fluctuations or droplets interact with the background and an applied external field. The energy needed to create one of these excitations with ℓ monomers is

$$H = h\ell + J\ell^{\frac{d-1}{d}}, \tag{3.19}$$

where h is the magnetic field and J is proportional to the spin-spin interaction. The first term in Eq. (3.19) is the interaction with the field and the second term is the interaction with the background. We want to calculate the free energy in the grand canonical ensemble. First consider the case for a fixed size ℓ of the droplets. The chemical potential μ is defined as $\partial E/\partial n$, where E is the total energy of interaction of the droplets of size ℓ with the field and background [Callen 1985]. Because the droplets are assumed to be non-interacting, the energy of n droplets of size ℓ is given by

$$E_\ell = \left(h\ell + J\ell^{\frac{d-1}{d}}.\right)n. \tag{3.20}$$

Hence the chemical potential for droplets of size ℓ is

$$\mu_\ell = h\ell + J\ell^{\frac{d-1}{d}}. \tag{3.21}$$

The activity z_ℓ is defined as

$$z_\ell \equiv e^{-\beta\mu_\ell}. \tag{3.22}$$

We can now calculate the grand canonical partition function Ω_ℓ for droplets of size ℓ.

$$\Omega_\ell = \sum_n \frac{z_\ell^n}{n!} Q_{nl}. \tag{3.23}$$

The term Q_{nl} is the canonical partition function of a system of n non-interacting droplets of size ℓ and hence equal to V^n where V is the volume of the system.

From Eq. (3.21)–(3.24b) we obtain

$$\Omega_\ell = \sum_n \frac{V^n}{n!} \exp\big[-\beta(h\ell + J\ell^{\frac{d-1}{d}})n\big] \tag{3.24a}$$

$$= \exp\big[\exp[-\beta(h\ell + J\ell^{\frac{d-1}{d}})V]\big]. \tag{3.24b}$$

The Gibbs free energy per unit volume for clusters of size ℓ is

$$\frac{1}{V}\ln\Omega_\ell = \exp\big[-\beta(h\ell + J\ell^{\frac{d-1}{d}}\big]. \tag{3.25}$$

Because the droplets are non-interacting, we can obtain the free energy per unit volume, $f(h, J)$, by summing over all droplet sizes.

$$f(h, J) = \sum_\ell \exp\big[-\beta(h\ell + J\ell^{\frac{d-1}{d}})\big] \tag{3.26}$$

Equation (3.26) gives the free energy for the classical droplet model. It is called classical because it assumes compact droplets. This assumption should be a reasonable if the system is not near any critical points.

We now define a variable t' in the same way we defined t in Eq. (3.16),

$$t' \equiv \frac{|h|^d}{J^d}\ell, \tag{3.27}$$

and restrict our considerations to $|h| \ll 1$. In this limit t' can be considered a continuous variable, and Eq. (3.26) can be written as

$$f(h, J) = \frac{J^d}{|h|^d}\int_0^\infty e^{-\frac{J^d}{|h|^{d-1}}(\alpha t' + t'^{\frac{d-1}{d}})} dt', \tag{3.28}$$

where α is the sign of h. For stable equilibrium $\alpha = 1$. We want to extend the model to study the metastable state. In the stable state the magnetic field term h produces an increase in the energy when a droplet is created. In the metastable state the magnetic field term produces a lowering of the energy when a droplet appears. Hence we take $h < 0$

in the metastable state or that $\alpha = -1$ in Eq. (3.28). Unfortunately for $\alpha = -1$ the sum in Eq. (3.26) or the integral in Eq. (3.28) does not converge, which makes sense physically because negative values of h should correspond to the "other" stable phase. However, the equilibrium state corresponding to negative values of h requires a change in the background which this model in its present form cannot accommodate. Nevertheless, this does not prevent the use of this model to describe the metastable state. Before discussing the formal aspects of this description we take another look at Eq. (3.26) for negative h.

The argument of the exponential in Eq. (3.26) is

$$\beta\big[|h|\ell - J\ell^{\frac{d-1}{d}}\big], \tag{3.29}$$

where we have taken $h < 0$. The sum over the droplet size ℓ causes the argument in Eq. (3.29) to decrease (become more negative) until $\ell = \ell_c$, where

$$\ell_c = \Big(\frac{d-1}{d}\Big)^d \Big(\frac{J}{|h|}\Big)^d. \tag{3.30}$$

The term ℓ_c is reminiscent of the critical size in the theory of nucleation in Chapter 1. Until $\ell = \ell_c$ the partition function sum in Eq. (3.26) has the properties of an equilibrium quantity. We see that one way to describe metastability in the droplet model context is to restrict the sum over ℓ to $\ell < \ell_c$, where ℓ_c defines the critical droplet.

There are still several questions that need to be considered. First, the restriction to $\ell < \ell_c$ is not unique. Why not truncate the sum at $2\ell_c$ or $\ell_c/2$? This question is valid and corresponds to a real physical ambiguity. There is a certain randomness to nucleation, and although a droplet may exceed the critical length ℓ_c and should grow, fluctuations can drive it back. The second question we must address is if we are to use the idea of a truncated sum, how do we relate the critical size ℓ_c at which we truncate the partition function sum to the nucleation rate? Also, how do we account for the dependence of the nucleation rate on temperature and dynamics seen in Figs. 3.1–3.3?

Following Langer [Langer 1967] we will take a different route to the metastable state which will make the connection between the critical droplet and the nucleation rate. Instead of setting $\alpha = -1$ in Eq. (3.28) suppose we analytically continue α from 1 to -1. We can keep the modulus of $\alpha = 1$ so we can set $\alpha = e^{i\theta}$. Although the integration can be done in the variables of Eq. (3.28), it will be more transparent if we define $z^d \equiv t'$. Equation (3.28) becomes

$$f(h, J) = \frac{dJ^d}{|h|^{d-1}} \int_0^\infty z^{d-1} e^{-\frac{J^d}{|h|^{d-1}}(\alpha z^d + z^{d-1})} dz. \tag{3.31}$$

To analytically continue $f(h, J)$ to negative h we set $z = \rho e^{i\phi}$. The integral in Eq. (3.31) will be done on a contour in the complex z plane such that the real part

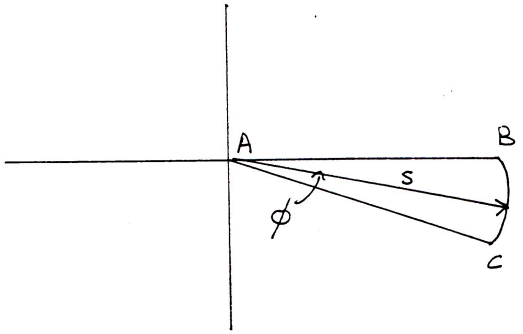

Figure 3.4: Contour used to analytically continue $f(h, J)$.

of αz^d is positive. In that way we will guarantee the convergence of the integral. This restriction implies that $\cos(\theta + d\phi) > 0$. Consider the integral over the contour in Fig. 3.4. From the Cauchy theorem the integral equals zero. Assume that $\theta = 0$. If ϕ is chosen such that $\cos(d\phi) > 0$, then the contribution over the semi-circular part of the contour vanishes as $s \to \infty$. Therefore the integral from A to B equals the integral from A to C. However, the integral from A to C converges over a different range of θ than the integral from A to B.

For example, suppose that $d = 2$ and $\phi = \pi/8$. Then for $\theta = 0$ the contribution over the semi-circular contour from B to C vanishes because the exponential in the integrand of Eq. (3.31) equals

$$e^{-\frac{J^d}{|h|^{d-1}}[\cos(2\phi)s^2+s]}, \tag{3.32}$$

and ϕ varies between 0 and $\pi/8$. Moreover the integral over the part of the contour between C and A also converges because $\cos(\pi/4) > 0$. However the integral over the A to C segment will converge for values of $\theta > 0$. We need only require that $\cos(\theta+\pi/4) > 0$ or $-\pi/2 < \theta+\pi/4 < \pi/2$. Therefore the integral over A to C converges for $-3\pi/4 < \theta < \pi/4$. Note that the integral over A to C will converge for $\theta = 0$ but will also converge for values of θ for which the integral over A to B will not. The integral over A to C is the analytic continuation of the integral over A to B. We can continue this process until $\theta = \pi$ and in this way analytically continue to $\alpha = -1$.

We could have also analytically continued by rotating θ to $-\pi$ which would have necessitated rotating the *contour* clockwise rather than the counter clockwise rotation depicted in Fig. 3.4. Note that for $\theta = \pi$ the range of ϕ is from $-3\pi/4$ to $-\pi/4$ in $d = 2$. For $\theta = -\pi$, ϕ ranges from $\pi/4$ to $3\pi/4$. The fact that these two ranges for ϕ do not overlap indicates that there is a branch point at $h = 0$ and we have put the branch cut on the negative real axis. There are two distict contours. One describes the rotation $\theta \to \pi_+$ and the other $\theta \to \pi_-$ For $\alpha = -1$ all terms in the integrand in (3.xx) are real except

of course z. We can chose our two seperate contours for the two different approaches to $\alpha = -1$ to be symmetric about the real axis. Therefore $f(|h|, J, \alpha \to -1_+)$ is the complex conjugate of $f(|h|, J, \alpha \to -1_-)$

As we discussed above we are working in the limit $h \sim 0$. Consequently the integral in Eq. (3.31) can be done with the method of steepest descent [Mathews and Walker 1965]. From Eq. (3.31) the saddle point is at

$$z_c = -\frac{d-1}{\alpha d}. \tag{3.33}$$

As α is rotated, the saddle point rotates in the complex z plane until for $\alpha = -1$ the saddle point is at $z_c = (d-1)/d$. To do the integrals corresponding to the analytic continuation we use the contours shown in Fig. 3.5.

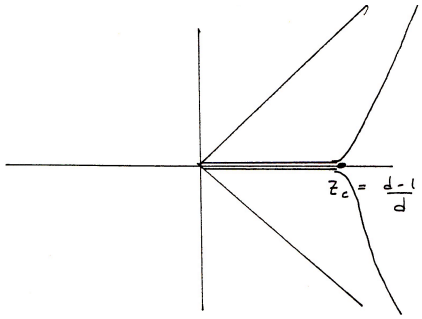

Figure 3.5: Steepest descent contours for analytic continuation.

The contours shown in Fig. 3.5 start at the origin, run along the real axis up to the saddle point, go down the path of steepest descent and asymptotically approach the lines drawn at $\phi = \pi/4 + \epsilon$ and $\phi = -\pi/4 - \epsilon$. Because two contours give free energies that are complex conjugates of each other, the real parts are the same. The difference in the two free energies $f(|h|, J, \alpha \to -1_+) - f(|h|, J, \alpha \to -1_-)$ is twice the imaginary part and is evaluated over the contour shown in Fig. 3.6. This countour is the difference of the two contours in Fig. 3.5.

It makes sense to consider the integral from the origin to the saddle point along the real axis in Fig. 3.5 as the metastable state free energy. The saddle point value of z corresponds to the critical droplet value of $\ell = \ell_c$. Hence the integral along the real axis up to z_c corresponds to the restricted partition function sum we discussed.

What is the physical significance of the imaginary part of the free energy? If we evaluate the integral in Eq. (3.31) over the contour shown in Fig. 3.6 using steepest [Mathews and Walker 1965], we obtain

$$2\,\mathrm{Im}\, f(|h|, J, \alpha \to -1_+) = M \frac{dJ^d}{|h|^{d-1}} \Big[\frac{d-1}{d}\Big]^{d-1} e^{-\frac{J^d}{k_B T |h|^{d-1}} \frac{(d-1)^{d-1}}{d^d}}, \tag{3.34}$$

where

$$M = \left[\frac{J^d \pi (d-1)^{d-1}}{k_B T |h|^{d-1} d^{d-2}} \right]^{-1/2} . \tag{3.35}$$

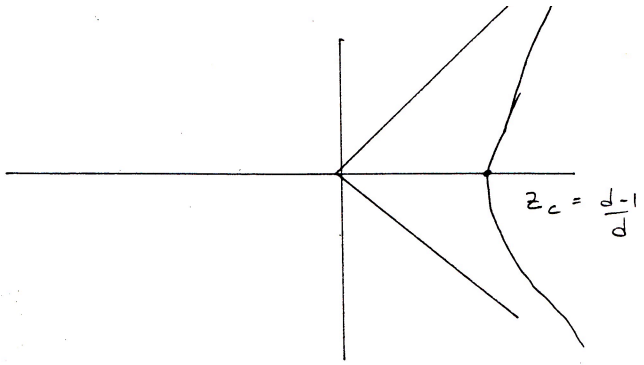

Figure 3.6: Contour for the imaginary part of the free energy in Eq. (3.34).

We can now compare Eqs. (3.34) and (3.35) with Eq. (3.18) obtained from the Becker-Döring theory. The first thing to notice is that the exponential terms in Eqs. (3.18) and (3.34) are the same. That is, the free energy cost of the critical droplet from the analytical continuation, Becker-Döring and the simple theory in Chapter 1 are dominated by the same exponential term. The second point is that the prefactor in Eq. (3.34), which includes the constant M in Eq. (3.35), is different than the prefactor in Eq. (3.18). Of course we are not referring to the replacement of σ in Eq. (3.18) by J in Eq. (3.34). The surface tension $\sigma \sim J$ for $T \ll T_c$ where we expect the classical droplet model to be accurate. We are referring to the different dependence on $|h|$ and J. From the discussion in Sec. 3.1 we might assume that the difference is due to the inclusion in the Becker-Döring theory of dynamical effects not included in the purely static analytical continuation. However, the similarity is striking. This similarity led Langer [Langer 1967] to conclude that at least a part of nucleation rate can be obtained from the analytical continuation of the free energy. This procedure is in many ways reminiscent of the relation between the lifetime of a resonance and the imaginary part of the scattering amplitude [Gottfried 1966]. We will pursue this point of view using the droplet model as a paradigm. When we convert these ideas into the language of scalar field theory, we obtain the most powerful technique presently available to describe the nucleation process.

Suggestions for Further Reading

D. W. Heermann, A. Coniglio, W. Klein, and D. Stauffer, "Monte Carlo simulation of metastable states in 3D Ising models," J. Stat. Phys. **36**, 447–470 (1984).

T. S. Ray and J. S. Wang, "Metastability and nucleation in Ising models with Swendsen-Wang dynamics," Physica A **167**, 580–588 (1990).

R. Swendsen and J. S. Wang, "Nonuniversal critical dynamics in Monte Carlo simulations," Phys. Rev. Lett. **58**, 86–88 (1987).

O. Penrose and J. L. Lebowitz, "Towards a rigorous molecular theory of metastability," in *Fluctuation Phenomena*, edited by E. W. Montroll and J. L. Lebowitz, North-Holland (1976) and references therein.

D. W. Heermann, W. Klein, and D. Stauffer, "Spinodals in long-range interaction systems," Phys. Rev. Lett. **47**, 1262 (1982).

C. Domb and N. W. Dalton, "Crystal statistics with long-range forces: I. The equivalent neighbour model," Proc. Phys. Soc. **89**, 859 (1966).

W. Klein and C. Unger, "Spinodals, pseudospinodals and nucleation," Phys. Rev. B **28**, 445 (1983). .

A. Coniglio and W. Klein, "Correlated site-bond percolation and Ising critical droplets," J. Phys. A **13**, 2775 (1980).

J. D. Gunton, M. San Miguel, and P. S. Sahni, "The dynamics of first order phase transitions," in *Phase Transitions and Critical Phenomena*, Vol. 8, edited by C. Domb and J. L. Lebowitz, Academic Press (1983).

Herbert B. Callen, *Thermodynamics and an Introduction to Thermostatistics*, 2nd ed., John Wiley & Sons (1985).

J. S. Langer, "Theory of the condensation point," Ann. Phys. (NY) **41**, 108 (1967).

J. Mathews and R. L. Walker, *Mathematical Methods of Physics*, Benjamin (1965).

K. Gottfried, *Quantum Mechanics, Vol. 1: Fundamentals*, Benjamin, (1966).